Research Square

Preprints are preliminary reports that have not undergone peer review.
They should not be considered conclusive, used to inform clinical practice,
or referenced by the media as validated information.

CB2R Agonist Reduces Astroglial and Microglial Reactions and Attenuates the Impact of Focal Cerebral Ischemia in Mice

Laura Romina Caltana

lcaltana@fmed.uba.ar

Universidad de Buenos Aires, Unidad Académica de Histología

Alicia Brusco

Universidad de Buenos Aires, Unidad Académica de Histología

Research Article

Keywords: CB2 receptor, CB2 receptor agonist, Cannabinoid system, Neuroprotection, cerebral ischaemia

Posted Date: May 11th, 2026

DOI: https://doi.org/10.21203/rs.3.rs-9533706/v1

License: This work is licensed under a Creative Commons Attribution 4.0 International License.
Read Full License

Additional Declarations: No competing interests reported.

Abstract

Therapeutic strategies to prevent the consequences of cerebral ischemia remain scarce. Given that the endocannabinoid system plays a neuromodulatory role in synaptic transmission, the cannabinoid system is gaining interest as a treatment target in different nervous system pathologies. Cannabinoid receptor type 1 (CB1R) is highly distributed in neurons and glial cells of the central nervous system (CNS), while cannabinoid receptor type 2 (CB2R) is mainly expressed in immune system cells and lowly expressed in neurons and glial cells of the CNS. In this work, we analyzed the effects of CB2R agonist for the treatment of focal brain ischemia by middle cerebral artery occlusion (MCAo) in C57Bl/6 mice. Animals received CB2R agonist JWH015 (4mg/kg), CB2R antagonist AM630 (1mg/kg) or vehicle 3, 24 and 48 hours after MCAo or sham operation. Neural deficit scores were obtained and motor tests were performed 1 day before and 3, 7 and 28 days after MCAo to assess motor activity. GFAP and MAP2 immunohistochemistry and tomato lectin staining were also carried out for morphological analysis of neurons, astrocytes, and microglia in the injured cerebral cortex. CB2R agonist JWH015 reduced MCAo-associated infarct size area, neuronal dendrite loss, astroglial hypertrophy and hyperplasia, while CB2R antagonist increased damage. Motor test data showed an improvement in motor activity after MCAo upon CB2R agonist treatment but not after antagonist treatment. In sum, this work provides further evidence that CB2R is involved in neuronal survival and the regulation of neuroprotection in a model of focal cerebral ischemia in mice and shows that CB2R agonist treatment reduces neuronal degeneration and astroglial and microglial reaction, thus ameliorating the motor activity deterioration following the ischemic event.

INTRODUCTION

Stroke is the second leading cause of death, responsible for approximately 11% of total deaths worldwide (www.who.int/) and with a global prevalence of 101.5 million people in 2019 (Virani et al., 2021). Stroke causes severe and lasting disability, particularly in elderly people, and can lead to loss of independence and the need for long-term care. Many efforts have been made by the scientific and clinical community to develop pharmaceutical agents that allow an effective treatment and thus reduce the significant deleterious effects. At the moment, blood flow restoration by intravenous injection of recombinant tissue plasminogen activator (tPA) is the gold standard treatment for ischemic stroke to be administered within 4.5 hours from the onset of symptoms (Doyle et al., 2008; Berge et al., 2021). It is currently thought that the best strategy should focus on addressing the development of neuroprotective therapies that include a reduction in glutamate levels, free radical production, and inflammation (Del Zoppo, 2006), all of which can induce brain hypothermia (Colbourne et al., 1997).

The potentially neuroprotective effects of cannabinoid receptor agonists on the CNS have been well established for years (Mechoulam et al., 2002; van der Stelt and Di Marzo, 2005). Cannabinoid receptor type 2 (CB2R) is widely expressed in cells of the immune system and has inflammatory regulatory functions (McKallip et al., 2002). Since the first evidence of the presence of CB2R in microglial cells, detected both in brain and primary cultures of rat microglial cells twenty years ago (Carlisle et al., 2002),

the expression of CB2R has been continuously studied in chronic inflammation and its upregulation has been postulated in microglial cells during inflammatory process due to intracerebral LPS injection (Concannon et al., 2015) and astrocytes (Fernandez-Trapero et al., 2017). The specific role of CB2R in inhibiting pro-inflammatory cytokine release is concentration-dependent (Correa et al., 2010). For example, the release of TNF is blocked by selective CB2R agonist JWH015 in inflammation models (Ehrhart et al., 2005). CB2R selective agonist, trans-caryophyllene, attenuated morphological deterioration and LDH release in mixed cortical cultures exposed to oxygen-glucose deprivation/re-oxygenation and reduces cerebral ischemic injury via activation of the AMPK-CREB pathway in rats (Choi et al., 2013). Activation of CB2R by JWH133 induces neurogenesis in ischemic hippocampus and the transformation of microglial phenotype into a neurotrophic phenotype after germinal matrix hemorrhage (Tang et al., 2017). Moreover, CB2R-positive microglial cells of the spinal cord are currently the object of studies focusing on the treatment of inflammatory hyperalgesia and multiple sclerosis (Maresz et al., 2005).

Based on the hypothesis that cannabinoids could act as neuroprotective agents in an ischemic event, this work aims to evaluate the effect of a CB2R agonist in a murine model of permanent middle cerebral artery occlusion (MCAo).

MATERIALS AND METHODS

1. Animals

Adult male C57/Bl6 mice (25–32 g) obtained from the animal facility at the National Center of Atomic Energy (Buenos Aires, Argentina) were used in this study. Mice were housed in a light- (12/12 h light/dark cycle), humidity- and temperature-controlled environment, with free access to standard laboratory rodent food and water. Animal treatments were in accordance with CICUAL protocols (Institutional Committee for the Care and Use of Laboratory Animals, School of Medicine, University of Buenos Aires, Number RES (CD) 2198 – 2015).

2. Mouse model of MCAo

Mice were deeply anesthetized with an intraperitoneal (i.p.) dose of ketamine/xylazine (100µg/g 10µg/g in 10ul saline) and the MCA was exposed and permanently occluded by electrocoagulation (Wagner et al., 2011; Liesz et al., 2009, modified for mice). The sham procedure was performed as described above except for the coagulation of the MCA (Control groups). The animal survival rate until the end of the experiments was 100% (for details, see Caltana et al., 2015).

3. Cannabinoid agonist/antagonist treatment

Adult mice were randomly assigned to six groups per recovery time 3, 24 and 48 hours after the surgical procedure and i.p. injected with CB2R agonist JWH015 (4mg/kg; Price et al., 2009) or CB2R antagonist

AM630 (1mg/kg; Hayakawa et al., 2007; Hayakawa et al., 2008). Both drugs were first dissolved in DMSO and diluted in saline. The control group was injected with the same volume of DMSO dissolved in saline solution at the same time points.

4. Behavioral tests on motor activity

4.1 Neurological score

Neurological examinations were performed on Day 1 (D1) 3 hours after the surgical procedure, D2- D4, D7, D14, D21 and D28 (Longa et al., 1989). The neurological findings were scored on a five-point scale: 0- no neurological deficit, 1- failure to fully extend left forepaw (a mild focal neurological deficit), 2- circling to the left (a moderate focal neurological deficit), 3- falling to the left (a severe focal deficit), 4- not walking spontaneously and a depressed level of consciousness.

4.2 Cylinder test

The cylinder test (Li et al., 2004) was adapted to be used in mice to assess forelimb use and rotation asymmetry. Each mouse was placed in a transparent cylinder, and forepaw exploration was assessed as the number of instances the animal used each paw to touch the cylinder. A total of 10 movements were recorded during the 10-minute test. The final score was calculated as: (non-impaired forelimb movement - impaired forelimb movement) / (non-impaired forelimb movement + impaired forelimb movement + both movements) as previously described in rats (Schallert et al., 2000).

4.3 Corner test

In the home cage, each mouse was placed between two boards measuring 30 cm x 20 cm x 1 cm. The edges of the two boards were attached at a 30º angle with a small opening along the joint to encourage entry into the corner. Each mouse was placed between the two angled boards facing the corner and halfway to the corner. When entering deep into the corner, both sides of the mouse vibrissae are simultaneously stimulated. The mouse then rears forward and upward, and then turns back to face the open end. Non-ischemic mice turn either left or right, but ischemic mice preferentially turn toward the non-impaired, ipsilateral (right) side. The turns in one versus the other direction were recorded from ten trials for each test. Turning movements that were not part of a rearing movement were not scored (Zhang et al., 2002).

4.4 Hanging wire

This test was used to assess asymmetry in the use of the forelimbs during vertical examination as a measure of forelimb capacity and strength. Animals were suspended by their forelimbs on a wire stretched between 2 columns at a height of 60 cm above a foam pillow. The time in seconds that each animal was suspended was recorded, with a score of zero when the mouse fell immediately and a maximum suspension time of 120 seconds. Two tests were performed for each mouse on each day of testing (Li et al., 2004).

4.5 Latency test

Each animal was placed on a flat surface, and the time it took to travel a distance equivalent to body length was recorded. Two trials were conducted, and the time recorded in each trial was averaged (Li et al., 2004).

5. Morphological analysis

After a recovery time of 7 or 28 days (D7 and D28), each animal was fixed by intracardiac perfusion with 4% paraformaldehyde in 0.1M phosphate buffer (PB), pH 7.4, and post-fixed for 4 hours in the same solution. Coronal sections of the brains were cut with a vibratome (25 µm) and stored in a 50% glycerol solution at -20°C.

5.1 Toluidine blue staining

Brain sections were rinsed with phosphate buffered saline (PBS) and distilled water and then incubated in Toluidine blue 0.5% (w/v) dissolved in sodium carbonate 2.5% (w/v). Sections were then dehydrated and coverslipped with Permount mounting media.

5.2 Fluoro-Jade® B staining procedure

Brain sections were mounted with distilled water onto gelatin coated slides and Fluoro-Jade® B (Millipore) staining was performed as previously described (Balan et al., 2006). Sections were examined with an epifluorescence microscope using a filter system suitable for the visualization of fluorescein or fluorescein isothiocyanate (FITC).

5.3 Immunohistochemistry stainning

Vibratome brain sections of animals belonging to the different experimental groups were simultaneously processed as previously described (Caltana et al., 2014). After PBS rinses, endogenous peroxidase activity was inhibited with 0.5% (v/v) H_2O_2 in PBS for 30 minutes at room temperature. Brain sections were then blocked for 1 hour with 3% (v/v) normal goat serum in PBS. After rinsing in PBS, sections were incubated for 48 hours at 4°C with the primary antibodies and then rinsed and incubated 1 hour at room temperature with biotinylated secondary antibodies (1:500). After further washing in PBS, sections were incubated for 1 hour with the Extravidin complex solution (1:400, Sigma). After washing five times in PBS and twice in 0.1 M acetate buffer, pH 6, the development of peroxidase activity was carried out with 0.035% (w/v) 3.3'-diaminobenzidine plus 2.5% (w/v) nickel ammonium sulfate and 0.1% (v/v) H_2O_2 diluted in acetate buffer. After enzymatic incubation, sections were washed with distilled water, dehydrated, and coverslipped using Permount.

All antibodies, as well as the Extravidin complex, were dissolved in PBS containing 1% (v/v) normal goat serum and 0.3% (v/v) Triton X-100, pH 7.4. Primary antibody dilutions were 1:3000 glial fibrillary acidic

protein (GFAP, Dako), 1:1000 microtubular associated protein-2 (MAP2, Sigma) and 1:500 rabbit anti-CB2R (Cell Signalling). Controls for the immunohistochemistry procedure were routinely performed by omitting the primary antibody. These control sections developed no immunohistochemical labeling.

5.4 Lectin staining

Brain sections were rinsed in PBS, and endogenous peroxidase activity was inhibited with 0.5% (v/v) H_2O_2 in PBS for 30 minutes at room temperature. Brain sections were blocked for 1 hour with 3% (v/v) normal goat serum in PBS. After rinsing in PBS, sections were incubated for 48 hours at 4°C with biotynilated lectin *Lycopersicon esculentum lectin* (6 ug/ml, Sigma; Caltana et al., 2009) and then rinsed and incubated 1 hour at room temperature with the Extravidin complex solution (1:400). After washing five times in PBS and twice in 0.1 M acetate buffer, pH 6, the development of peroxidase activity was carried out with 0.035% (w/v) 3,3-diaminobenzidine plus 2.5% (w/v) nickel ammonium sulfate and 0.1% (v/v) H_2O_2 diluted in acetate buffer. Following the enzymatic incubation step, sections were washed with distilled water, dehydrated, and coverslipped with Permount.

6. Morphometric digital image analysis

Images were acquired on an Axiolab epifluorescence microscope (Carl Zeiss) equipped with a Q-Color3 CCD camera (Olympus). Counting and morphometry were performed using Image Pro PLUS 4.5 (Media Cybernetics) and Image J (NIH, http://rsb.info.nih.gov/ij/) software.

The brain area analyzed was the primary motor cortex (M1/M2) (Franklin and Paxinos, 2007). In each coronal section, each microscopic field was selected within the limits of the ischemic penumbra to be morphometrically analyzed. Cell counting was performed for lectin + and Fluorojade B+ cells, whereas the GFAP immunoreactive area was measured for astrocytes. For MAP2-positive fibers, the total area of the immunolabeled fibers was relativized to the total area of the corresponding microscopic field (20x primary magnification), rendering a relative area parameter. The lesioned ischemic area was estimated as a fraction of the total contralateral hemisphere.

7. Statistical analysis

For motor tests, reported values represent the mean ± standard deviation (SD) of experiments performed. Differences among the means of the six groups were statistically analyzed by two-way analysis of variance (ANOVA). Dunnett's multiple comparison tests were conducted following the significance/non-significance of the overall ANOVA. Statistical significance was set to $p < 0.05$.

Three separate immunohistochemical experiments were carried out for each immunostaining study. Individual experiments comprised 6 to 10 coronal sections of each animal from each group. Five to ten fields were measured from each brain area in each coronal section of each animal by stereological analysis. Reported values represent the mean ± standard deviation (SD) of experiments performed for

each marker and each brain area. Differences among the means of the six groups were statistically analyzed by one-way analysis of variance (ANOVA). Dunnett's multiple comparison tests were conducted following the significance/non-significance of the overall ANOVA. Statistical significance was set to $p < 0.05$ using GraphPad Prism v5.00 software (GraphPad Software Inc.).

Animals groups were codified and were experiments were analyzed in blind conditions.

RESULTS

1. CB2R expression was upregulated after MCAo

In normal conditions, CB2R is mainly expressed in cells of the immune system, although evidence also supports CB2R expression in neurons (Gong et al., 2006; Brusco et al., 2008). In this work, the expression of CB2R was analyzed on D1, D2, D3 after MCAo in animals with no further treatment. Control animals showed CB2R expression in cells with microglial morphology, while MCAo animals showed higher expression of CB2R in microglial cells and also in astrocytes (Fig. 1A). This higher expression of CB2R was restricted to the regions close to the ischemic lesion, and CB2R-positive astrocytes were located surrounding the blood vessels, which suggests a role for CB2R in bloodstream regulation (Fig. 1B, C and D).

2. Selective CB2R agonist JWH015 reduced neurological deficits after MCAo

To evaluate the neurological effects of brain ischemia, the neurological score was determined on D1, D2, D3, D4, D7, D14, D21 and D28 in MCAo and control sham-operated mice. On D1, no significant differences were observed in control groups, while MCAo produced an increase in the neurological scale which was reversed by JWH015 treatment. AM630-treated animals presented a neurological scale value significantly higher than the Saline-Control group (Fig. 2). As from D2, a significant increase was detected in the neurological scale value in MCAo groups which remained until D28. JWH015 treatment reduced the neurological scale value, rendering no differences from the Control-Saline group. The MCAo-Saline and MCAo-AM630 groups showed a significantly higher neurological scale value than the Control-Saline group (Fig. 2).

3. Selective CB2R agonist JWH015 reduced motor alterations after MCAo

Motor activity tests were carried out on D0 (before surgery), to obtain a baseline value, and on D4, D7, D14, D21 and D28 after MCAo.

Cylinder test

No significant differences were observed in control groups. In contrast, the MCAo-Saline group showed an increase in the number of turns to the right, as did the MCAo-AM630 group from D4 to D28. The MCAo-JWH015 group showed no significant differences with respect to the Control-Saline group (Fig. 3A).

Corner test

The non-ischemic control groups exhibited no significant differences from the Control-Saline group (Fig. 3B). The MCAo-Saline and MCAo-AM251 groups showed a significant increase in turns to the right with respect to the Control-Saline group as from D7 which was maintained until D28. MCAo-JWH015 animals showed no differences from Control-Saline group, whereas the MCAo-AM630 group showed a significant increase in turns to the right at D28 (Fig. 3B).

Hanging wire and latency

Control-JWH015 and Control-AM630 animals showed no significant differences with respect to the Control-Saline group in the time they remained suspended by their forelimbs, while the MCAo groups showed progressive deterioration in forelimb strength (Fig. 4A). In addition, MCAo did not produce a deterioration in movement latency compared to the Control-Saline group. The MCAo-JWH015 group showed a deterioration in this parameter on D4, D7, D14 and D21 and D28 (Fig. 4B).

4. Selective CB2R agonist JWH015 reduced the size of the lesion after MCAo

The area of damaged tissue was calculated in serial brain sections stained with Toluidine blue. The ipsilateral injured area and the total area of the contralateral hemisphere were measured, and the relationship between these values was considered the percentage of the damaged hemisphere ipsilateral to the MCAo (Fig. 5A). Results showed that the area injured by MCAo was significantly reduced after JWH015 treatment as compared to the MCAo-Saline and MCAo-AM630 groups (Fig. 5B).

5. Selective CB2R agonist JWH015 reduced the number of degenerating neurons and prevented the loss of dendritic arborization after MCAo

Fluoro Jade B is an anionic fluorochrome capable of selectively staining degenerated neurons in brain slices. The technique detects neuronal degeneration and stains neuronal bodies, dendrites, axons, and axon terminals of degenerated neurons (Fig. 6A). Assays showed that the damage produced by MCAo promoted neuronal degeneration, while treatment with CB2R agonist JWH015 significantly reduced the number of degenerated neurons as compared to the MCAo-Saline and MCAo-AM630 groups (Fig. 6B).

In addition, MCAo induced a reduction in dendritic processes which was greater after treatment with CB2R antagonists. The area covered by MAP2 + processes evaluated in primary motor cortex (M1) areas sensitive to hypoxia induced by MCAo (Fig. 7A) showed no significant differences across control groups

(Fig. 7A, B). On D7, MCAo produced a significant reduction in MAP2 + neuronal processes which remained after treatment with CB2R antagonists. No significant differences were detected in MCAo groups treated with CB2R agonist JWH015 as compared to the Control-Saline group (Fig. 7B). On D28, no significant differences were observed in the area covered by MAP2 + fibers in the Control groups, except for Control-AM630. MAP2 + processes were reduced in the groups undergoing MCAo but recovered with JWH015 treatment (Fig. 7C).

6. Selective CB2R agonist JWH015 reduced astroglial reaction after MCAo

Mature astrocytes have a special type of intermediate filaments in the cytoskeleton: GFAP is more abundant in fibrous than in protoplasmic astrocytes and is the main determinant of astrocyte shape and the extension of characteristic cytoplasmic processes (Ham and Cormack, 1986; Jones and Cowan, 1986). In the present work, GFAP and the area covered by GFAP+ processes were used as parameters of astrocyte reaction produced by MCAo (Fig. 8A).

On D7, no variations were recorded in the area covered by GFAP+ astrocytes in the control groups (Fig. 8A, B). In contrast, MCAo produced reactive astrocytosis, which was greater in the MCAo-AM630. No differences were detected in the MCAo groups treated with JWH015 as compared to the Control-Saline group.

On D28, control groups showed no significant differences in the area covered by astrocytes. MCAo produced an increase in astrocyte area which remained in the groups treated with AM630 but was reduced in the groups treated with JWH-015 (Fig. 8A, C).

7. Selective CB2R agonist JWH015 reduced the number of microglial cells after MCAo

Microglial cells are the resistant macrophages of the CNS. Resting microglial cells have small cell bodies and multiple thin processes which give them a stellate morphology. Upon nervous tissue injury, microglial cells change their morphology, becoming amoeboid (Rodriguez et al., 2010). In this work, the number of microglial cells with stellate and amoeboid morphology was analyzed through tomato lectin staining (Fig. 9A).

On D7, no changes in the number of microglial cells with stellate morphology were found in the cortex in control groups, except in the group treated with CB2R antagonist. MCAo produced a significant increase in the number of microglial cells with stellate morphology which was maintained in the groups treated with AM630 but was offset in the groups treated with JWH015 (Fig. 9A, B). Moreover, MCAo produced an increase in the number of amoeboid microglial cells which did not decrease after AM630 treatment but returns to Control-Saline values after treatment with JWH015.

On D28, alterations were only observed in the number of stellate microglial cells in the ischemic group treated with AM630 (Fig. 9A, C). Regarding amoeboid microglial cells on D28, no differences were detected across control groups; however, a significant increase was observed after MCAo which was only compensated by JWH015 treatment (Fig. 9C).

DISCUSSION

CB2R has demonstrated its anti-inflammatory activity and neuroprotective properties in numerous experimental studies, with the benefit of having no psychotropic effects like those of CB1R agonists (Lutz 2020). Interestingly CB2R activation infarct size and restore cognitive functions in a photoinjury model of a permanent ischemia but could be detrimental in learning and memory processes in sham-animals (Ronca et al., 2015).

While low in basal conditions in healthy brains (Ashton et al., 2007; Brusco et al., 2008a; Brusco et al., 2008b; Ashton et al., 2014; Rathod et al., 2023), CB2R expression is upregulated in different models of acute and chronic brain injury such us chronic pain, Alzheimer's disease, multiple sclerosis, and ischemia (Luongo et al., 2010; Lopez et al., 2018; Benito et al., 2008; Ashton and Glass, 2007; Komorowska-Müller et al., 2021). Upregulation of brain CB2R appears to be an adaptive response to various insults from the CNS. CB2R mRNA expression is gradually increased from day 1 to day 5 after stroke in rats, consistent with this IBA1 mRNA expression (Yu et al., 2015). We show an increased in CB2R expression between D1 and D3 after MCAo, mostly observed in the areas surrounding the ischemic core, both in cells with microglial and astrocytic morphology. In addition, blood vessels also evidenced CB2R expression, probably due to the expression of presence of CB2R in the vascular feet of blood-brain barrier astrocytes. Accordingly, our study included a treatment of various CB2R agonist doses that coincided with the days in which CB2R increased its expression after ischemia.

In 2007, Zhang and collaborators demonstrated the neuroprotective effects of CB2R agonists O-1966 and O-3853 after 24h of ischemic transient insult, reducing infarct volume, improving motor activity, and decreasing leukocyte/endothelial interactions (Zhang et al., 2007). CB2R knockout mice show larger cerebral infarction and worse neurological function compared to wild type mice (Zhang et al., 2009).

Here, we amplify the study during 28 days after permanent ischemia. In addition, we analyzed neuronal damage and astrocytic and microglial reaction parameters. Improvement in motor parameters, such as lower neurological scores and a decrease in contralateral motor alterations, in tests carried out up to 28 days post-MCAo in animals treated with CB2R agonist JWH015, while those treated with selective antagonist AM630 showed equally altered or even exacerbated motor parameters after MCAo.

Different cardiac ischemic models have also proven CB2R agonist JWH133 to be effective in reducing the area of cardiac infarction, probably due to the inhibition of oxidative stress and neutrophil infiltration and the activation of the ERK 1/2 and STAT3 pathways (Montecucco et al., 2009). CB2R activation reduces heart dysfunction and the levels of cardiac injury markers associated with remarkable inhibition of inflammatory cell infiltration and fibrosis (Liu et al., 2020). In a photothrombosis model induced in

mice, CB2R agonist β-caryophyllene combined with cannabidiol showed that the reduction of Iba-1 positive microglial cells is related with decreased infarct size (Yokubaitis et al., 2021).

In line with this evidence, our results showed a reduction in cerebral infarct size upon JWH015 treatment and a concomitant decrease in neuronal degeneration and alterations in dendritic arborization. Of note, increased or prolonged neuroinflammation processes induce irreversible damage that can lead to neuronal degeneration or even neuronal death, which highlights the importance of reducing neuroinflammation upon nerve tissue damage (Komorowska-Müller and Schmöle, 2021).

CB2R activation can reduce the pro-inflammatory reaction and increase the expression of anti-inflammatory molecules. For instance, the pharmacological activation of CB2Rs with anandamide increases the expression of anti-inflammatory markers and decreases inflammatory ones (Correa et al., 2010), while the inhibition of CB2R generates the opposite effect (Mecha et al., 2015). CB2R activation also reduces the secretion of pro-inflammatory cytokines by microglia and their phagocytic activity (Ehrhart et al., 2005). CB2R stimulation following an intracerebral infusion of thrombin attenuated brain edema, preserved brain blood barrier (Li et al., 2015; Li et al., 2018). Moreover, CB2R suppression by AM630 increased inflammatory cytokines in hippocampus in neuroinflammatory response induced by generalized tonic–clonic seizures (Karan et al., 2021).

JWH133, a selective CB2R agonist, reduce infarct volume and improve neurological score when was administered 10min after permanent middle cerebral artery occlusion (Zarruk et al., 2012). Moreover, CB2R agonist JWH133 reduced neurological deficits and brain edema in subarachnoid hemorrhage in rats (Fujii et al., 2014). Authors also report the downregulation of IL-10 and TGF-β and support that CB2R activation induce anti-inflammatory effects driving microglial cells toward inactivated state. In addition, we observed both on D7 and D28 post MCAo, astrocytic reaction decreased with CB2R agonist treatment but remained increased with CB2R inhibition. Similar results were obtained for microglial cells, with an increase on D7 in the number of microglial cells and a predominance of amoeboid over stellate morphology which was only offset by JWH015. Moreover, the number of microglial cells remained increased on D28 in animals without treatment and those treated with CB2R antagonist, which demonstrates that CB2R stimulation reduces the inflammatory process through the inhibition of cell recruitment and microglial activation.

As other authors reported previously, CB2R agonists exert neuroprotective actions after ischemia, restoring motor activity and reducing inflammation in animal models of impaired cerebral blood flow. Here we also demonstrate that CB2R agonists reduce neuronal death and alterations in the dendritic tree, decrease the astrocytic and microglial reaction, in the long term after ischemia.

In conclusion, ischemia triggers a cascade of events that ultimately leads to neuronal degeneration and death. This in turn generates an increase in inflammation and astrocyte reaction which brings about even more neuronal death and the consequent deterioration in motor functions. In this scenario, our study demonstrates that selective treatment with a CB2R agonist after MCAo reduces the associated damage and promotes an improvement in motor performance. These findings unveil the selective activation of

CB2R as a therapeutic tool to accompany blood flow restoration therapies and thus reduce neurological disabilities produced by ischemic damage.

Declarations

Animal treatments were conducted in accordance with CICUAL protocols (Institutional Committee for the Care and Use of Laboratory Animals, School of Medicine, University of Buenos Aires; approval number RES (CD) 2198-2015).

Conflict of Interest

The authors declare that the research was conducted in the absence of any commercial or financial relationships that could be construed as a potential conflict of interest.

Contribution to the Field Statement

The cannabinoid system has become a potential tool for the treatment of various pathologies. In this study, we focus on type 2 cannabinoid receptor (CB2R) and its effect in a model of cerebral ischemia due to occlusion of the middle cerebral artery. Our encouraging findings show that treatment with JWH15, a selective CB2R agonist, after the ischemic event promotes a decrease in the size of infarct, in the number of degenerated neurons, and in astrocyte and microglia activation. Furthermore, the lower damage observed in nervous tissue is consistent with an improvement in motor skills observed in ischemic mice treated with the CB2R agonist. These data are consistent with a reduction in the inflammatory process reported for CB2R and suggest that treatment with CB2R agonists might become a therapeutic tool in ischemic processes.

Author Contribution

LC conducted all the steps in the experimental protocol, data processing, statistical analysis, and writing of the initial draft of the article. AB designed the experimental model, supervised the course of experiments, and wrote the final version of the article. LC and AB revised the final version of the article.

Acknowledgments

This work was supported by grants from Universidad de Buenos Aires (UBACYT 20020170100371BA) and FONCYT (PICT2017-0610), Argentina.

Data Availability

All data supporting the findings of this study are available from the corresponding author upon request.

References

erebroprotective action via a cannabinoid receptor-independent myeloperoxidase-inhibiting mechanism. J Neurochem. 2007;102(5):1488-1496. doi: 10.1111/j.1471-4159.2007.04565.x.
https://www.who.int/news-room/fact-sheets/detail/the-top-10-causes-of-death

Jones EG, Cowan WM. Tejido nervioso. In Histología. Weiss L (ed.). El Ateneo, Buenos Aires. 1986. Chapter 8: pp 258-337.

Karan AA, Spivak YS, Gerasimov KA, et al. CB2 receptors modulate seizure-induced expression of pro-inflammatory cytokines in the hippocampus but not neocortex. Mol Neurobiol. 2021;58(8):4028-4037. doi: 10.1007/s12035-021-02395-w.

Komorowska-Müller JA, Rana T, Olabiyi BF, Zimmer A, Schmöle AC. Cannabinoid Receptor 2 Alters Social Memory and Microglial Activity in an Age-Dependent Manner. Molecules. 2021 Oct 2;26(19):5984. doi: 10.3390/molecules26195984

Komorowska-Müller JA, Schmöle AC. CB2 Receptor in Microglia: The Guardian of Self-Control. Int J Mol Sci. 2020;22(1):19. doi: 10.3390/ijms22010019.

Li L, Tao Y, Tang J, et al. A Cannabinoid Receptor 2 Agonist Prevents Thrombin-Induced Blood-Brain Barrier Damage via the Inhibition of Microglial Activation and Matrix Metalloproteinase Expression in Rats. Transl Stroke Res. 2015;6(6):467-77. doi: 10.1007/s12975-015-0425-7.

Li L, Yun D, Zhang Y, et al. A cannabinoid receptor 2 agonist reduces blood-brain barrier damage via induction of MKP-1 after intracerebral hemorrhage in rats. Brain Res. 2018;1697:113-123. doi: 10.1016/j.brainres.2018.06.006.

Li X, Blizzard KK, Zeng Z, et al. Chronic behavioral testing after focal ischemia in the mouse: functional recovery and the effects of gender. Exp Neurol. 2004;187(1):94-104. doi: 10.1016/j.expneurol.2004.01.004.

Liesz A, Hagmann S, Zschoche C, et al. The spectrum of systemic immune alterations after murine focal ischemia: immunodepression versus immunomodulation. Stroke. 2009;40(8):2849-58. doi:10.1161/STROKEAHA.109.549618.

Liu X, Zhang D, Dong X, et al. Pharmacological activation of CB2 receptor protects against ethanol-induced myocardial injury related to RIP1/RIP3/MLKL-mediated necroptosis. Mol Cell Biochem. 2020;474(1-2):1-14. doi: 10.1007/s11010-020-03828-1.

Longa EZ, Weinstein PR, Carlson S, et al. Reversible middle cerebral artery occlusion without craniectomy in rats. Stroke. 1989;20(1):84-91. doi: 10.1161/01.str.20.1.84.

López A, Aparicio N, Pazos MR, et al. Cannabinoid CB2 receptors in the mouse brain: relevance for Alzheimer's disease. J Neuroinflammation. 2018;15(1):158. doi: 10.1186/s12974-018-1174-9.

Luongo L, Palazzo E, Tambaro S, et al. 1-(2',4'-dichlorophenyl)-6-methyl-N-cyclohexylamine-1,4-dihydroindeno[1,2-c]pyrazole-3-carboxamide, a novel CB2 agonist, alleviates neuropathic pain through functional microglial changes in mice. Neurobiol Dis. 2010;37(1):177-85. doi: 10.1016/j.nbd.2009.09.021.

Maresz K, Carrier EJ, Ponomarev ED, et al. Modulation of the cannabinoid CB2 receptor in microglial cells in response to inflammatory stimuli. J Neurochem. 2005;95(2):437-45. doi: 10.1111/j.1471-4159.2005.03380.x.

McKallip RJ, Lombard C, Fisher M, et al. Targeting CB2 cannabinoid receptors as a novel therapy to treat malignant lymphoblastic disease. Blood. 2002;100(2):627-34. doi: 10.1182/blood-2002-01-0098.

Mecha M, Feliú A, Carrillo-Salinas FJ, et al. Endocannabinoids drive the acquisition of an alternative phenotype in microglia. Brain Behav Immun. 2015;49:233-45. doi: 10.1016/j.bbi.2015.06.002.

Mechoulam R, Panikashvili D, Shohami E. Cannabinoids and brain injury: therapeutic implications. Trends Mol Med. 2002;8(2):58-61. doi: 10.1016/s1471-4914(02)02276-1.

Montecucco F, Lenglet S, Braunersreuther V, et al. CB(2) cannabinoid receptor activation is cardioprotective in a mouse model of ischemia/reperfusion. J Mol Cell Cardiol. 2009;46(5):612-20. doi: 10.1016/j.yjmcc.2008.12.014.

Price DA, Martinez AA, Seillier A, et al. WIN55,212-2, a cannabinoid receptor agonist, protects against nigrostriatal cell loss in the 1-methyl-4-phenyl-1,2,3,6-tetrahydropyridine mouse model of Parkinson's disease. Eur J Neurosci. 2009;29(11):2177-86. doi: 10.1111/j.1460-9568.2009.06764.x.

Rathod SS, Agrawal YO, Nakhate KT, Meeran MFN, Ojha S, Goyal SN. Neuroinflammation in the Central Nervous System: Exploring the Evolving Influence of Endocannabinoid System. Biomedicines. 2023;11(10):2642. doi: 10.3390/biomedicines11102642.

Rodríguez JJ, Witton J, Olabarria M, et al. Increase in the density of resting microglia precedes neuritic plaque formation and microglial activation in a transgenic model of Alzheimer's disease. Cell Death Dis. 2010;1(1):e1. doi: 10.1038/cddis.2009.2.

Ronca RD, Myers AM, Ganea D, et al. A selective cannabinoid CB2 agonist attenuates damage and improves memory retention following stroke in mice. Life Sci. 2015;138:72-7. doi: 10.1016/j.lfs.2015.05.005.

Schallert T, Fleming SM, Leasure JL, et al. CNS plasticity and assessment of forelimb sensorimotor outcome in unilateral rat models of stroke, cortical ablation, parkinsonism and spinal cord injury. Neuropharmacology. 2000;39(5):777-87. doi: 10.1016/s0028-3908(00)00005-8.

Tang J, Miao H, Jiang B, et al. A selective CB2R agonist (JWH133) restores neuronal circuit after Germinal Matrix Hemorrhage in the preterm via CX3CR1+ microglia. Neuropharmacology. 2017;119:157-169. doi: 10.1016/j.neuropharm.2017.01.027.

van der Stelt M, Di Marzo V. Cannabinoid receptors and their role in neuroprotection. Neuromolecular Med. 2005;7(1-2):37-50. doi: 10.1385/NMM:7:1-2:037.

Virani SS, Alonso A, Aparicio et al. Heart Disease and Stroke Statistics-2021 Update: A Report From the American Heart Association. Circulation. 2021;143(8):e254-e743. doi: 10.1161/CIR.0000000000000950.

Wagner DC, Riegelsberger UM, Michalk S, et al. Cleaved caspase-3 expression after experimental stroke exhibits different phenotypes and is predominantly non-apoptotic. Brain Res. 2011;1381:237-42. doi: 10.1016/j.brainres.2011.01.041.

Yokubaitis CG, Jessani HN, Li H, et al. Effects of Cannabidiol and Beta-Caryophyllene Alone or in Combination in a Mouse Model of Permanent Ischemia. Int J Mol Sci. 2021;22(6):2866. doi: 10.3390/ijms22062866.

Yu SJ, Reiner D, Shen H, et al. Time-Dependent Protection of CB2 Receptor Agonist in Stroke. PLoS One. 2015;10(7):e0132487. doi: 10.1371/journal.pone.0132487.

Zarruk JG, Fernández-López D, García-Yébenes I, et al. Cannabinoid type 2 receptor activation downregulates stroke-induced classic and alternative brain macrophage/microglial activation concomitant to neuroprotection. Stroke. 2012;43(1):211-9. doi: 10.1161/STROKEAHA.111.631044.

Zhang L, Schallert T, Zhang ZG, et al. A test for detecting long-term sensorimotor dysfunction in the mouse after focal cerebral ischemia. J Neurosci Methods. 2002;117(2):207-14. doi: 10.1016/s0165-0270(02)00114-0.

Zhang M, Adler MW, Abood ME, et al. CB2 receptor activation attenuates microcirculatory dysfunction during cerebral ischemic/reperfusion injury. Microvasc Res. 2009;78(1):86-94. doi: 10.1016/j.mvr.2009.03.005.

Zhang M, Martin BR, Adler MW, et al. Cannabinoid CB(2) receptor activation decreases cerebral infarction in a mouse focal ischemia/reperfusion model. J Cereb Blood Flow Metab. 2007;27(7):1387-96. doi: 10.1038/sj.jcbfm.9600447.

Figures

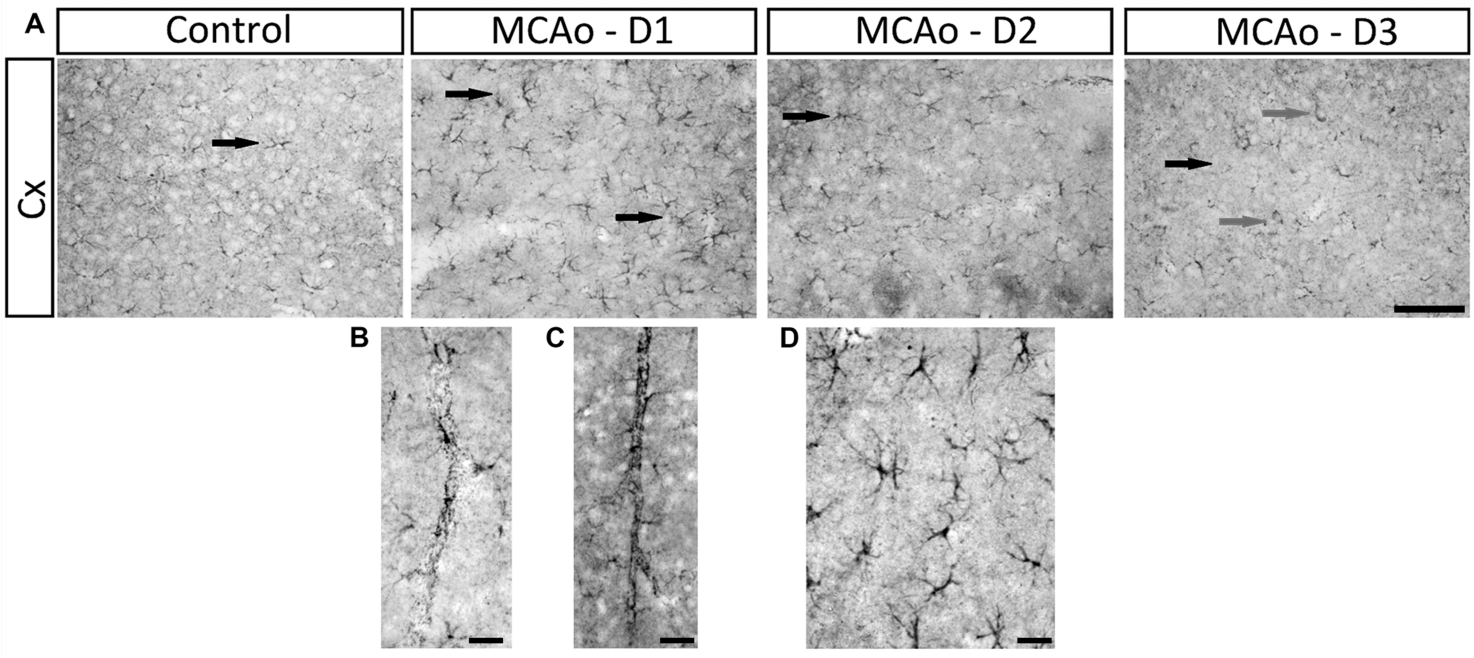


Figure 1

CB2R expression after MCAo. A. CB2R expression on D0-D3. Scale bar= 30mm. B and C. CB2R is expressed in astrocytes and blood vessels. Scale bar= 15mm. D. CB2R is expressed in astrocytes. Scale bar=15mm. Cx: cerebral cortex

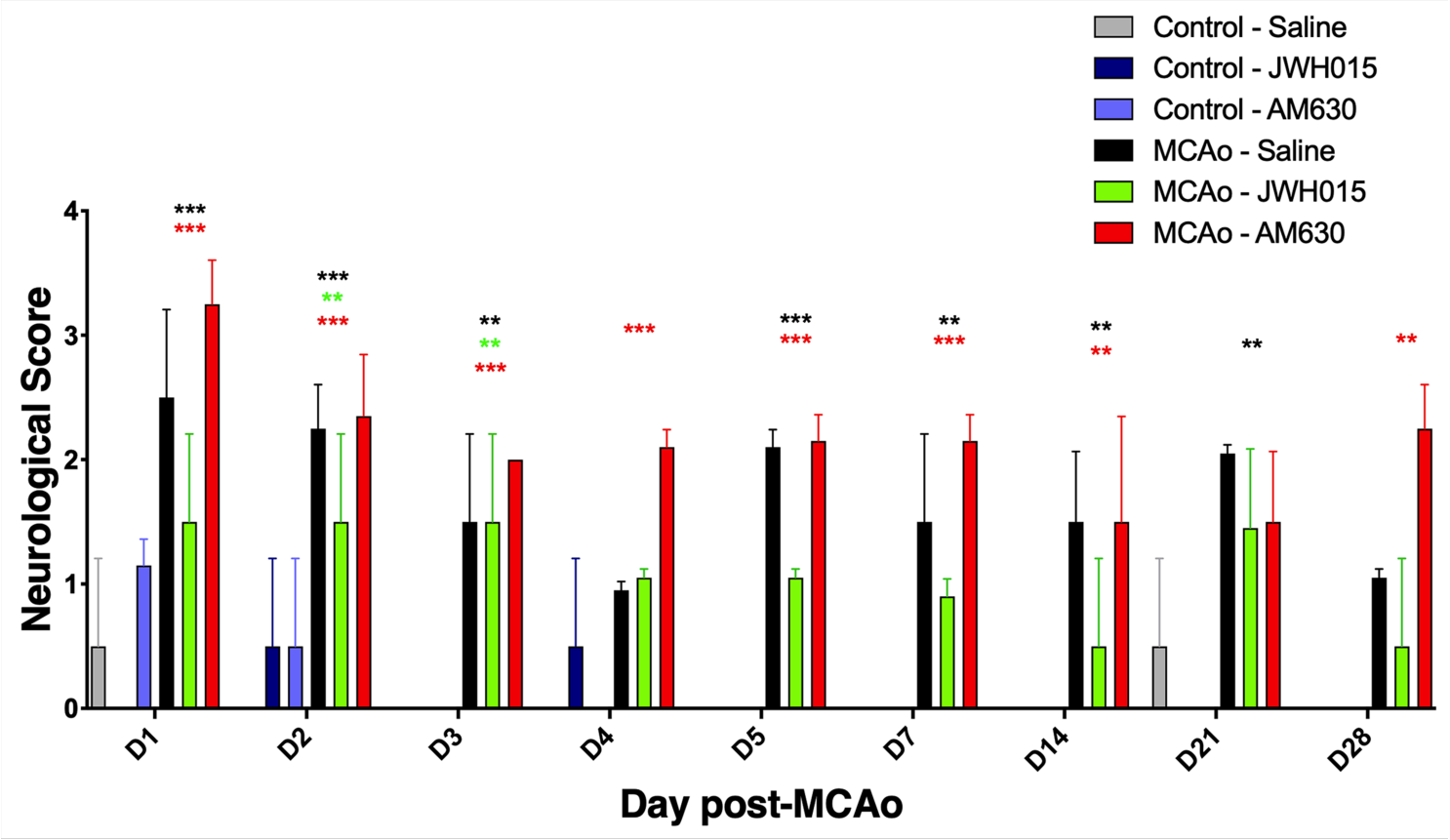


Figure 2

Neurological score after MCAo and agonist/antagonist treatment. Significance between treatments after two-way ANOVA and Dunnett's post-test. * p<0.05***; ** p<0.01; p<0.001. Comparisons were made to Control-Saline group. Asterisk colors correspond to: Black-MCAo-Saline group; Green-MCAo-JWH015 group; Red-MCAo-AM630 group. n= 10 per group

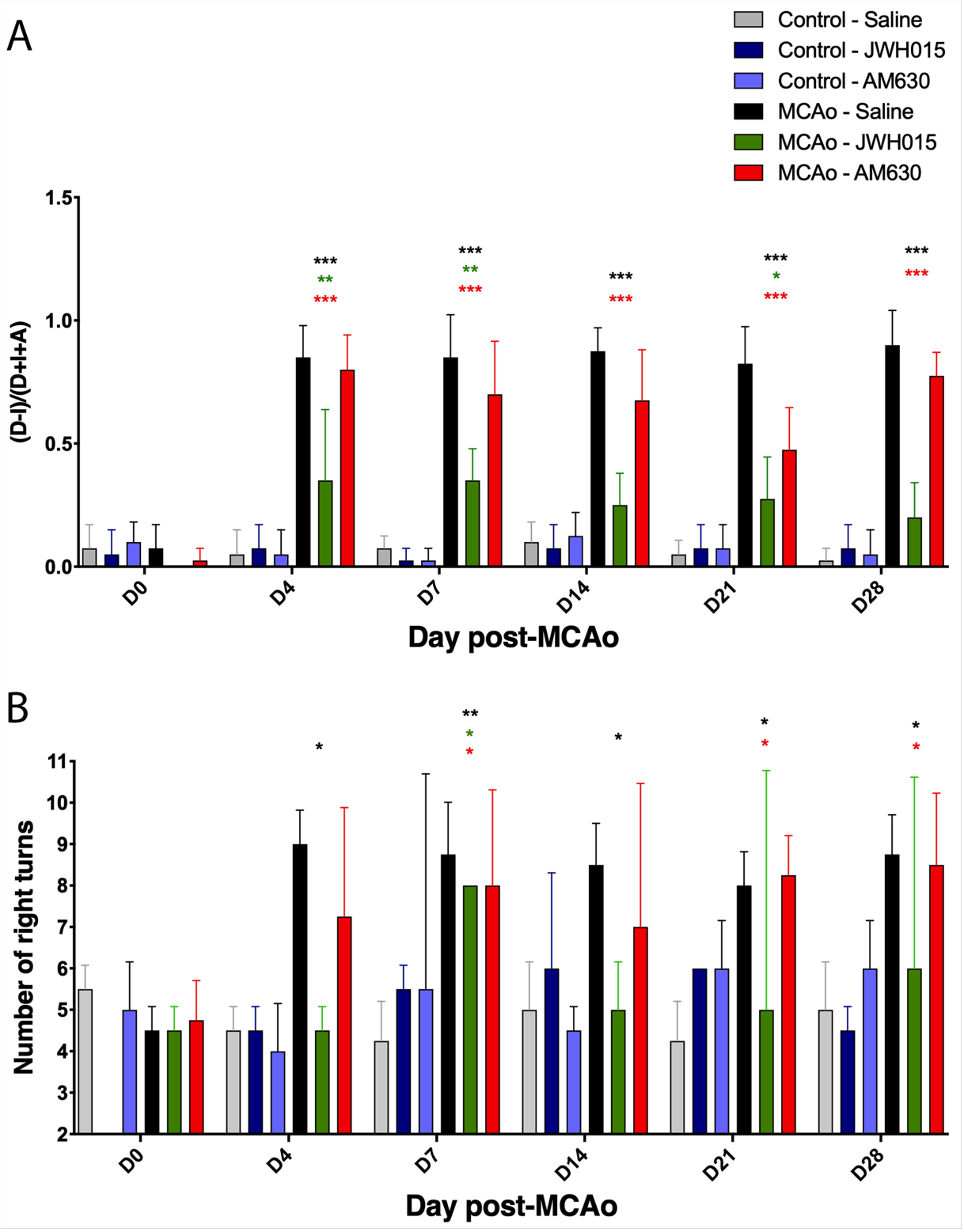


Figure 3

Motor activity after MCAo and agonist/antagonist treatment. A. Cylinder test. B. Corner test. Significance between treatments after two-way ANOVA and Dunnett's post-test. * p<0.05***; ** p<0.01; p<0.001. Comparisons were made to Control-Saline group. Asterisk colors correspond to: Black-MCAo-Saline group; Green-MCAo-JWH015 group; Red-MCAo-AM630 group. n= 10 per group

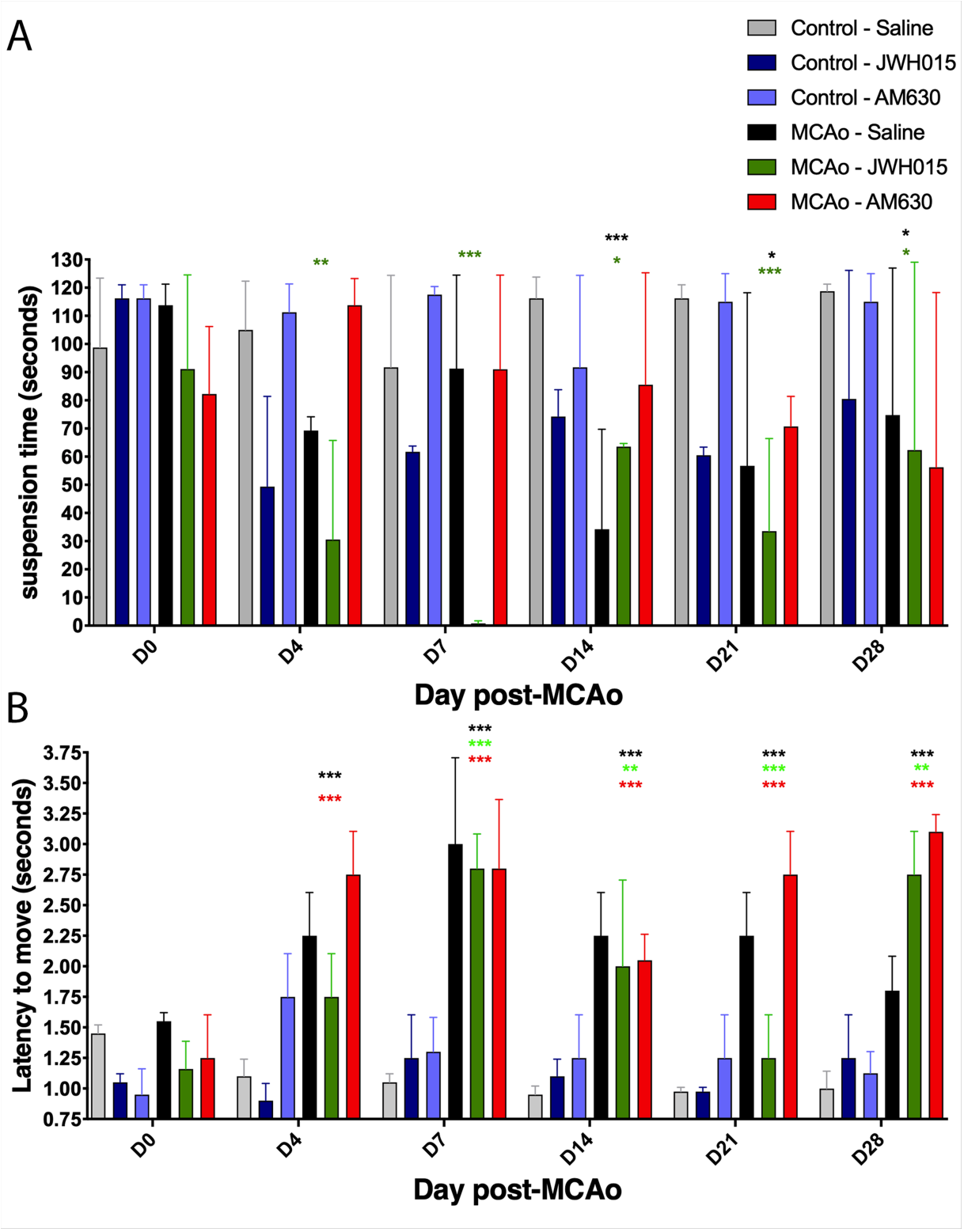


Figure 4

Motor activity after MCAo and agonist/antagonist treatment II. A. Hanging wire. B. Latency to move. Significance between treatments after two-way ANOVA and Dunnett's post-test. * p<0.05***; ** p<0.01; p<0.001. Comparisons were made to Control-Saline group. Asterisk colors correspond to: Black-MCAo-Saline group; Green-MCAo-JWH015 group; Red-MCAo-AM630 group. n= 10 per group

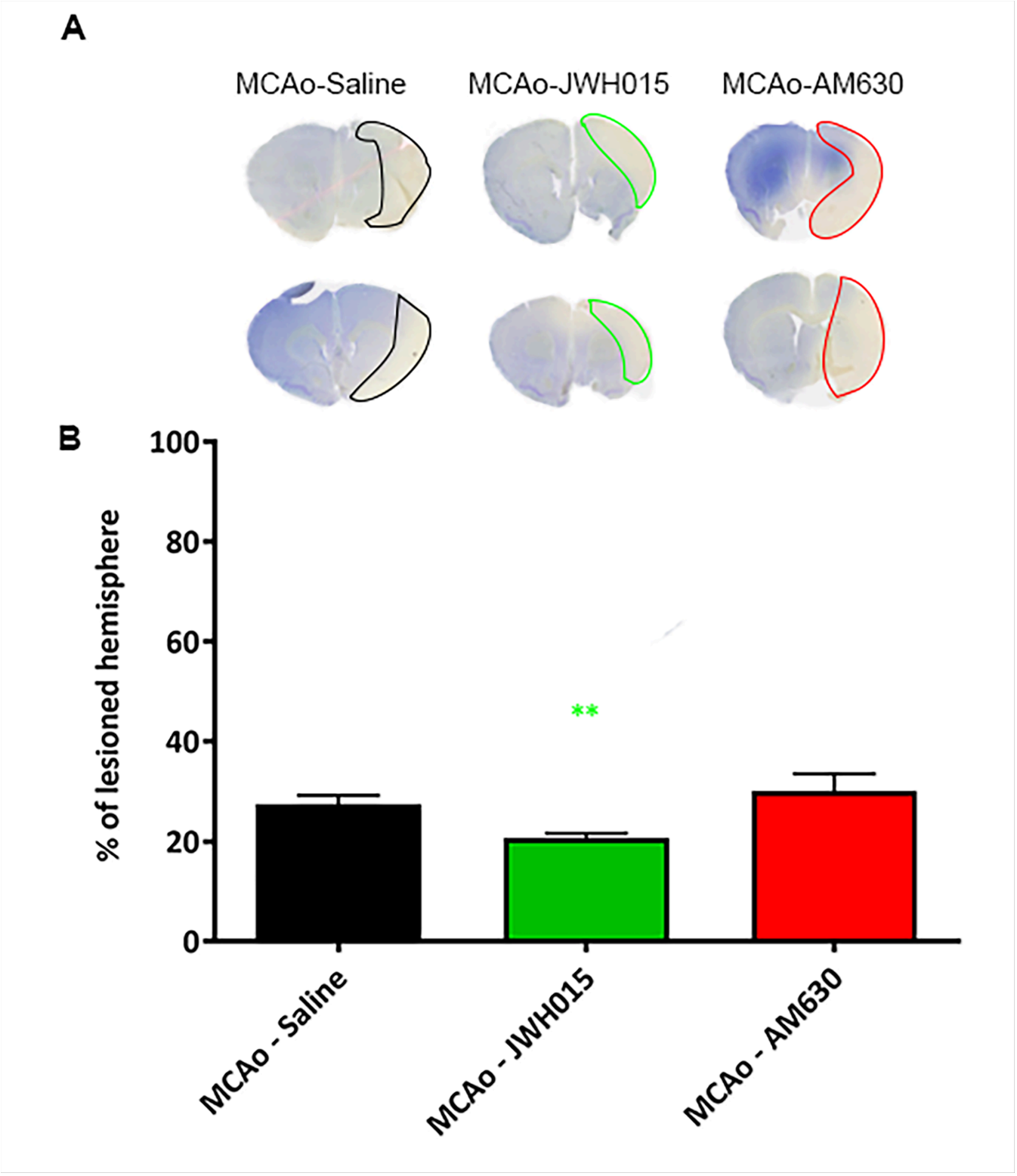


Figure 5

Lesion size after MCAo and agonist/antagonist treatment. A. Schematic representation. B. Percentage of lesioned hemisphere. Significance between treatments after one-way ANOVA and Dunnet post-test. **p<0.01 Comparisons were made to Control-Saline group. n= 5 per group.

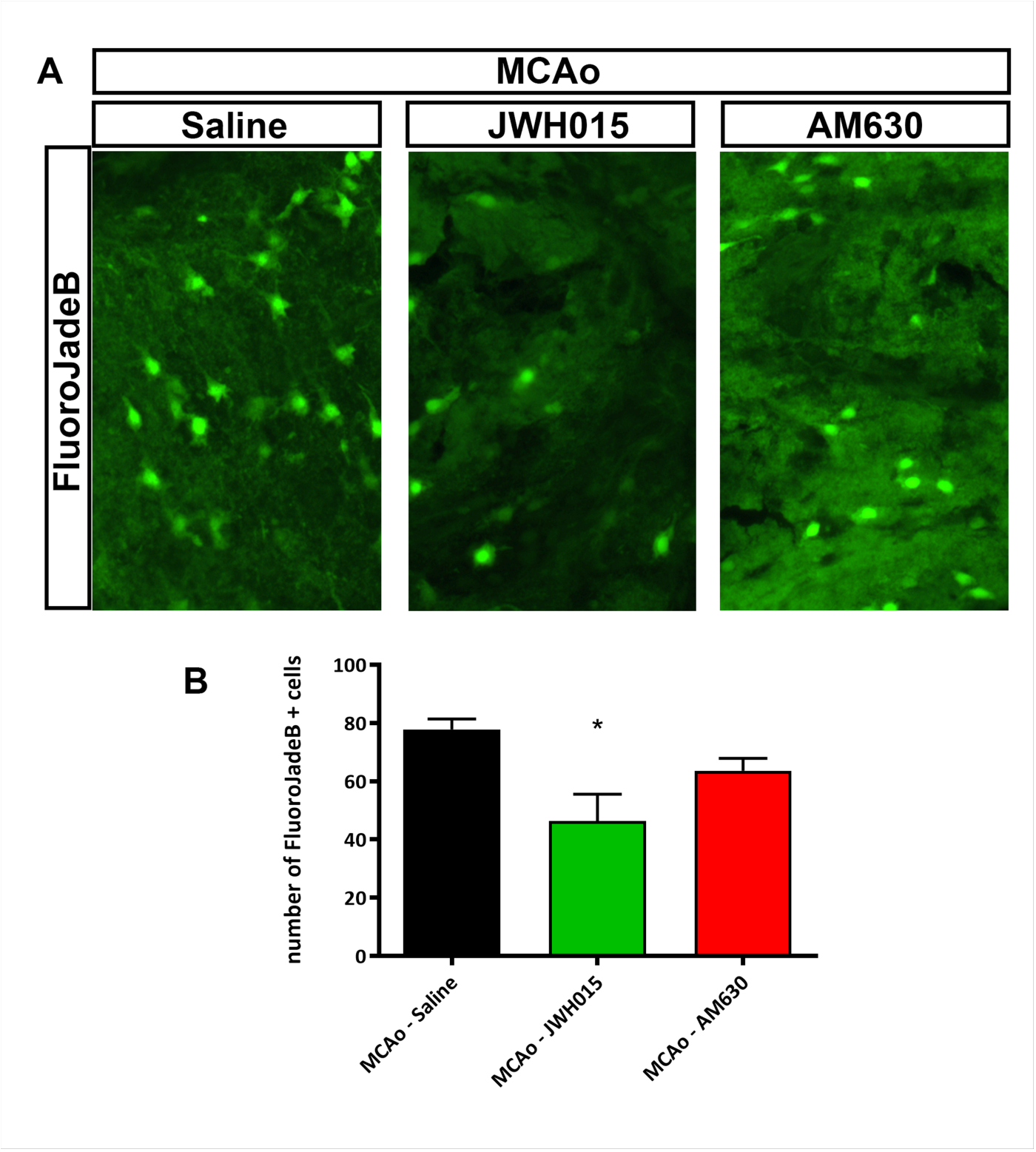


Figure 6

Neuronal degeneration after MCAo and agonist/antagonist treatment on D7. A. Fluorojade B staining in the ischemic penumbra in cerebral cortex. B. Representative scheme of the ischemic injury where the ischemic core and the penumbra are observed. The measurements were made in the penumbra area. C. Number of Fluorojade B+ cells after treatment. Significance between treatments after one-way ANOVA

and Dunnett's post-test. * p<0.05. Comparisons were made to Control-Saline group. n= 4-5 per group. Scale bar= 30mm

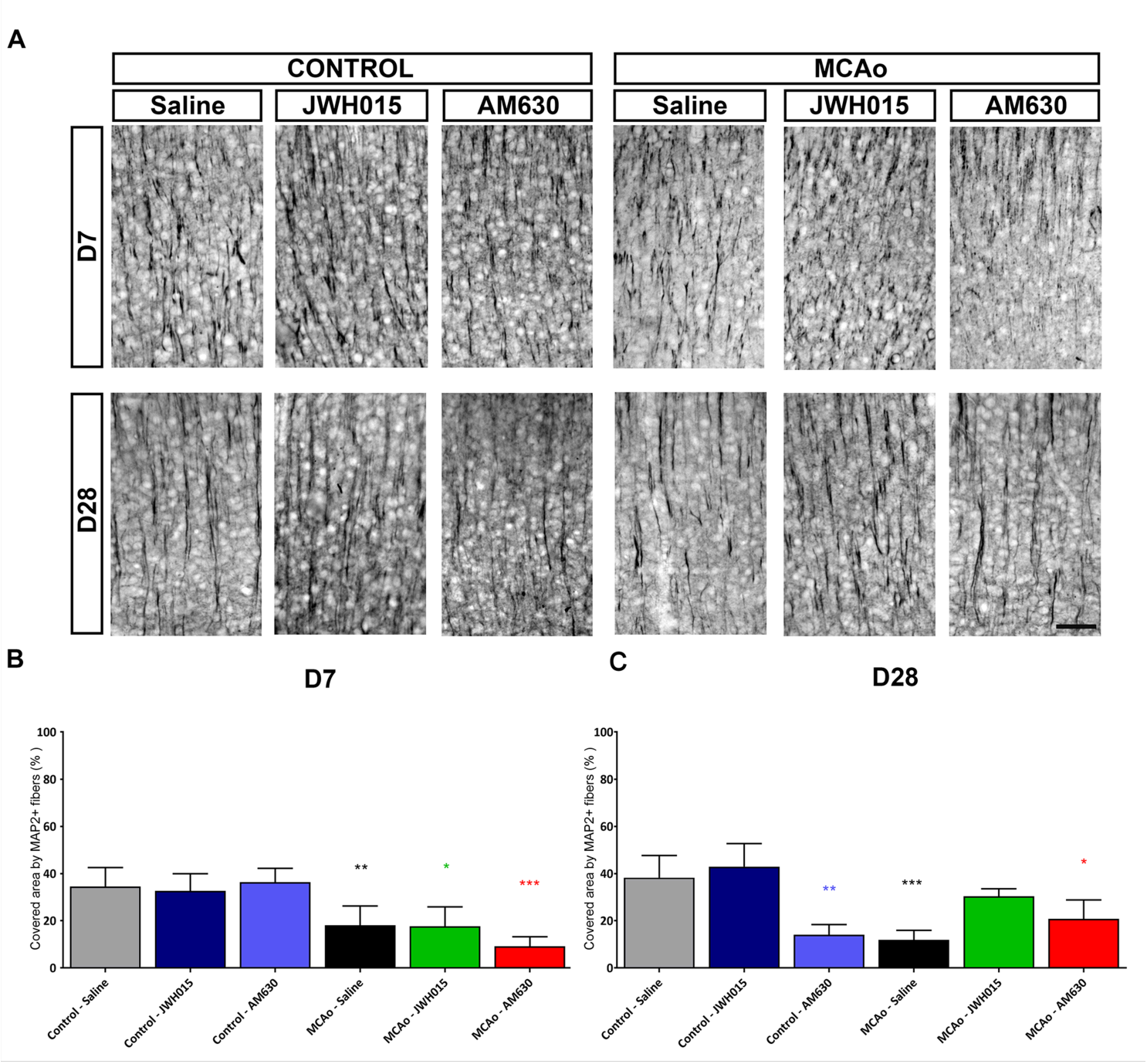


Figure 7

Dendritic arborization after MCAo and agonist/antagonist treatment. A. MAP2 immunostaining. B. Area covered by MAP2+ fibers on D7. C. Area covered by MAP2+ fibers on D28. Significance between treatments after one-way ANOVA and Dunnett's post-test. * p<0.05; ** p<0.01; ***p<0.001. Comparisons were made to Control-Saline group. n= 4-5 per group. Scale bar= 30mm

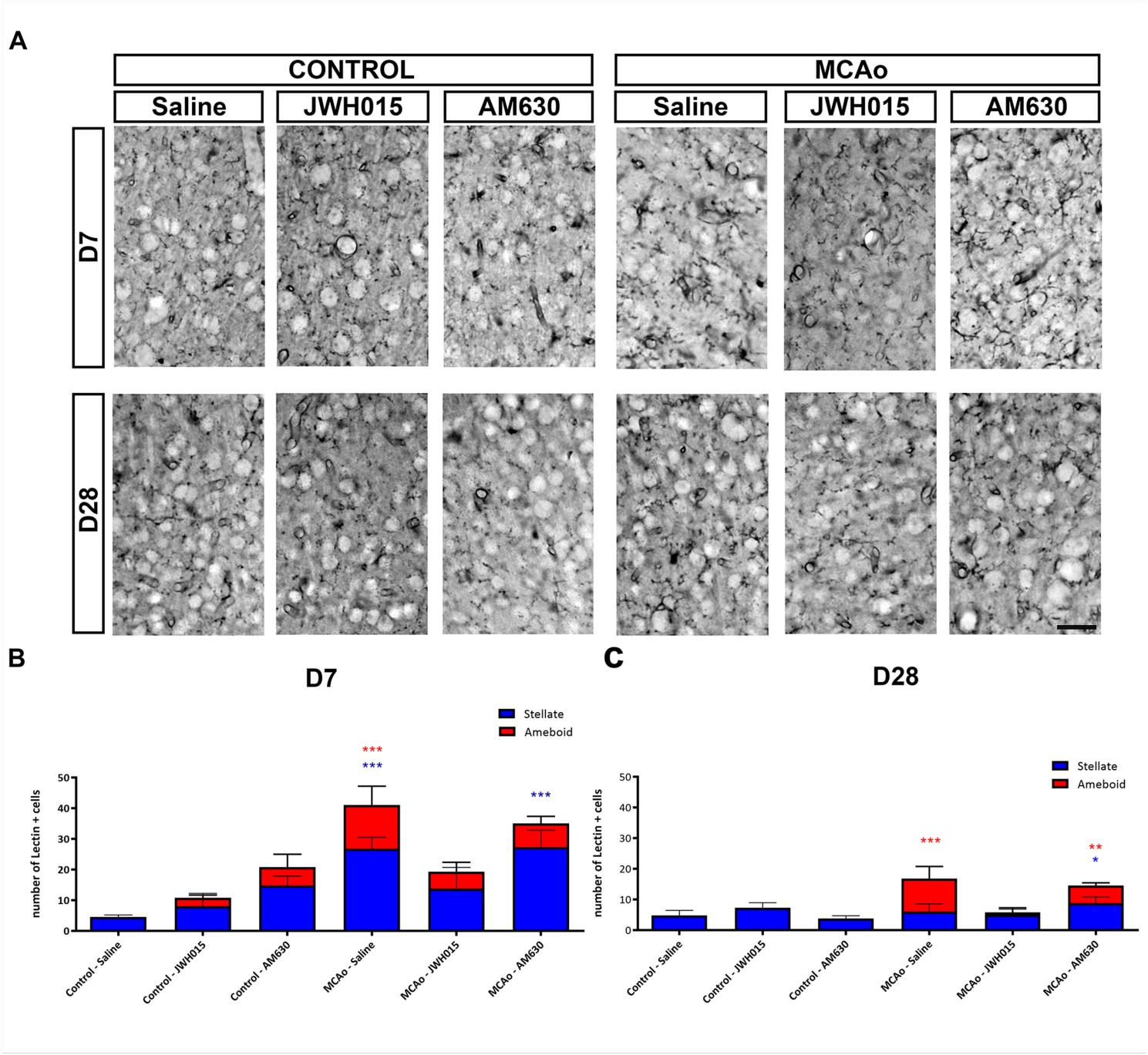


Figure 8

Astrocyte activation after MCAo and agonist/antagonist treatment. A. GFAP immunostaining. B. Area covered by GFAP+ astrocytes on D7. C. Area covered by GFAP+ astrocytes on D28. Significance between treatments after one-way ANOVA and Dunnett's post-test. * $p<0.05$; ** $p<0.01$; ***$p<0.001$. Comparisons were made to Control-Saline group. n= 4-5 per group. Scale bar= 30mm

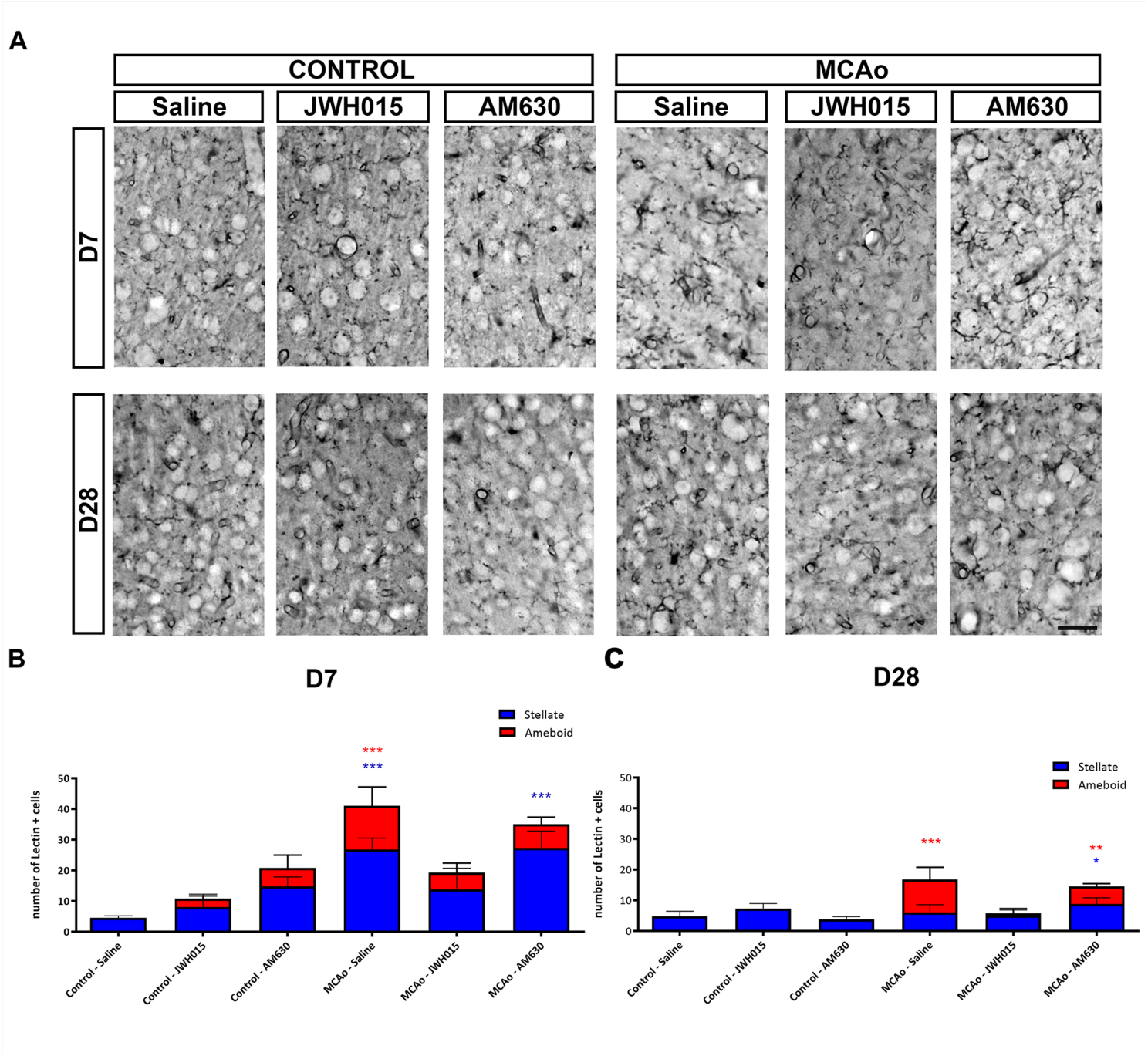


Figure 9

Microglial number and morphology after MCAo and agonist/antagonist treatment. A. Lectin staining. B. Number of lectin+ cells on D7. C. Number of lectin+ cells on D28. Bars in blue and red represent stellate cell and ameboid cell counting, respectively. Significance between treatments after one-way ANOVA and Dunnett's post-test. * p<0.05; ** p<0.01; ***p<0.001. Comparisons were made to Control-Saline group. n= 4-5 per group. Scale bar= 30mm